Quantitative methods in ocular fundus imaging: Analysis of retinal microvasculature.

Demetrio Labate, Basanta R. Pahari, Sabrine Hoteit, Mariachiara Mecati

Abstract Several diseases including diabetes, hypertension and glaucoma are known to cause alterations in the human retina that can be visualized non-invasively and in vivo using well established techniques of fundus photography. Since the treatment of these diseases can be significantly improved with early detection, methods for the quantitative analysis of fundus imaging have been the subject of extensive studies. Following major advances in image processing and machine learning during the last decade, a remarkable progress is being made towards developing automated quantitative methods to identify image-based bio-markers of different pathologies. In this paper, we focus on the automated analysis of alterations of retinal microvasculature - a particular class of structural alterations of special importance for early detection of hypertension, diabetic retinopathy and some neurological diseases.

Key words: retina imaging; representation learning; segmentation

1 Introduction

The retina is a layered tissue covering the interior part of the eye that is responsible for image formation. Since its function requires it to receive direct light from the outside world, the retina is uniquely accessible for imaging noninvasively and in vivo. In

Demetrio Labate
University of Houston, USA e-mail: dlabate@math.uh.edu

Basanta R. Pahari
University of Houston, USA e-mail: brpahari@math.uh.edu

Sabrine Hoteit
University of Houston, USA e-mail: sabrina@math.uh.edu

Mariachiara Mecati
Politecnico di Torino, Italy e-mail: mariachiara.mecati@polito.it

addition, the retinal tissue is metabolically active and, as an extension of the central nervous system, it exhibits a close affinity to the brain tissue in terms of anatomy, functionality and response to insult [2, 63, 79]. It follows that not only diseases of the eye but also circulatory and neurological diseases can manifest in the retina and several studies have demonstrated that retinal alterations may be predictive of a range of diseases of the eye (e.g., diabetic retinopathy, glaucoma) as well as other important systemic diseases (e.g., hypertension, stroke and Alzhaimer's disease), making retinal imaging a major subject of investigation.

Due to its importance for monitoring the health status of the eye, retinal imaging has a long history and photographic techniques were already applied at the end of the 19-th century [42]. Retinal fundus photography, in particular, was originally introduced by Gullstrand in 1910 [45] to visually record the rear of the eye, also known as the *fundus*. As successive studies have established the importance of retinal imaging to detect not only disease of the eye but also a range of systemic diseases, fundus photography has developed very rapidly. Due to its safety, cost effectiveness and non-invasive nature, this imaging tool has become a mainstay of the eye clinical care and it is now widely employed for large scale, population-based screening. Despite the emergence of new imaging modalities, the technology of fundus photography is still evolving and a new generation of inexpensive, portable, easy-to-operate fundus cameras is revolutionizing retinal screening programs and becoming widely available [80].

Evaluation of fundus images for medical diagnostics requires expert clinicians whose time is valuable and whose judgement is necessarily subjective. As a consequence, reliable automated approaches to retinal image analysis are in great need not only to improve diagnostic accuracy but also to increase clinician productivity in routine population screening settings. In response to this need, multiple methods have been proposed and implemented with focus on the segmentation of blood vessels in retinal fundus images, quantification of their alterations and detection of abnormalities. Since assessing the type and degree of such alterations or abnormalities is critical to detect the presence of a disease or discriminate among different diseases, targeted image analysis methods have been designed to reconstruct the vessel structure of the retina and extract anatomic landmarks including the macula, the fovea and the optic disc [2, 81].

While the literature on retinal image analysis is extensive (over 750 papers published to date) and includes a number of excellent reviews [2, 14, 81], in this paper, we focus specifically on the analysis of retinal microvascularization and computerized methods designed to quantify corresponding morphological changes in fundus images. Alterations in retinal microvascularization are known to correlate with the insurgence of diabetic retinopathy and cardiovascular diseases such as hypertension as well as brain diseases, since changes in retinal microvasculature may reflect similar changes occurring in cerebral microvasculature [16]. To reliably detect and accurately classify such vascular changes, a number of algorithms have been proposed that apply a variety of methods from statistics, classical and fractal geometry as well as neural networks. The goal of this paper is to survey conventional and

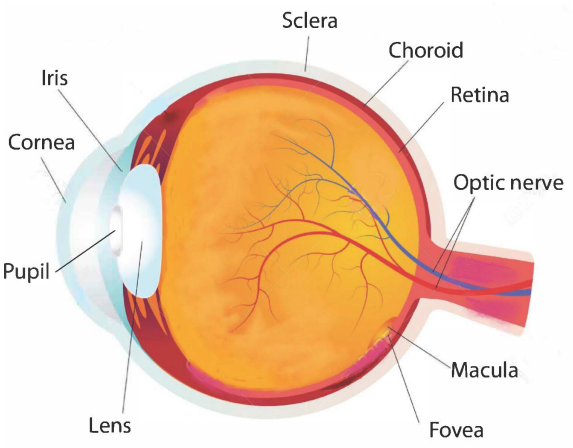

Fig. 1 Anatomy of the eye. The eye is our organ of sight and it consists of several components including the cornea, iris, pupil, lens, sclera, retina, macula, fovea, choroid and optic nerve. The retina is a tissue lining the inner surface of the posterior region of the eye.

state-of-the-art methods in this active area of investigation with special focus on emerging ideas from multiscale representations and deep learning.

The rest of the paper is organized as follows. In Sec. 2 we present some background material on the anatomy on the retina and fundus photography. In Sec. 3 we review the existing literature on the analysis of retinal microvascularization and illustrate the application of emerging techniques to this task including most notably methods from deep learning and advanced multiscale representations.

2 Anatomy of the retina and retinal imaging

We briefly review the anatomy of the retina and how retinal imaging is useful to detect and monitor a range of diseases.

2.1 Anatomic structure of the retina

We start with some notes about the anatomy of the retina and refer to [32, 59, 78] for additional details.

The retina is a thin (about 0.5 mm thick) transparent tissue lining the inner surface of the posterior region of the eye. It is composed of multiple layers of specialized sensory neurons that are interconnected through synapses. Light that enters the eye is captured by photoreceptor cells (the so-called *rod* and *cones* cells) located in the outermost layer of the retina and then converted into an electrical signal that eventually reaches the retinal ganglion cells. The axons of these cells form the *optic nerve* and, through this nerve, electrical signals are relayed to the higher visual processing centres that enable us to perceive visual images.

The central region of the retina (see Figure 1) contains an oval shaped pigmented region called *macula* that is responsible for the fine, high resolution vision. This region is thicker than peripheral retina due to the higher density of photoreceptors, especially cones, and their associated bipolar and ganglion cells as compared with peripheral retina. The *fovea*, located near the center of the macula, is a small pit containing the largest concentration of cone cells.

As for any other tissue, the retina receives blood through the vascular system and this system is visible from from the pupil, as in ophthalmoscopy or retinal photography. There are two sources of blood supply to the retina: the *central retinal artery* and the *choroidal blood vessels*. The choroidal blood vessels carry most of the blood flow and are responsible for the maintenance of the outer retina and the photoreceptors; the rest of the blood flows to the retina through the central retinal artery from the optic nerve head to nourish the inner retinal layers. The central retinal artery has four main branches that are clearly visible in retinal photography (see Figure 2) where the vessels emerging from the optic nerve head are displaced in a radial fashion curving toward and around the fovea.

2.2 Retinal manifestations of disease

Many diseases manifest themselves in the retina [2, 65] including not only diseases of the eye, such as glaucoma, age-related macular degeneration and diabetic retinopathy, but also cardiovascular diseases, such as hypertension and atherosclerosis, and brain diseases such as Alzheimer's disease. In fact, the retinal vascular network is optimized for efficient flow and alterations from this state that are observed on fundus images may be indicative of vascular damage and manifestation of disease processes. Such alterations may include: changes in morphological characteristics of the blood vessels, e.g., changes in thickness and tortuosity; blood vessel abnormalities, e.g., hemorrhages, microaneurysms, neovascularizations; abnormalities of the pigment epithelium, e.g., drusen; choroidal abnormalities, e.g., choroidal lesions. Critical problems are how to detect saddle changes that may be associated with early stages of a disease and how to discriminate alterations associated with different diseases.

2.3 Fundus photography.

As indicated above, fundus photography has been a seminal tool for the early developments in diagnoses of eye conditions and is still the most widely used in clinical practice. It requires a fundus camera consisting of an optical system comprising a specialized low power microscope with an attached camera capable of simultaneously illuminating and imaging the rear of the eye; this includes the retina, posterior pole, optic disc and macula [43]. Initially designed as a film-based imaging system, more recently, with the emergence of digital imaging, the use of digital cameras in

fundus photography has allowed to achieve more flexibility in image manipulation, faster processing and easier transmission of information. During the last decade, the technology of fundus photography has further developed and a new generation of inexpensive, portable, easy-to-operate fundus cameras has become widely available [80].

One main limitation of fundus photography is that generates a 2-D representation of the 3-D retinal tissue projected onto the imaging plane and, thus, it is not very effective to resolve the vessels located in the deeper retinal layers. Optical coherent tomography (OCT), introduced in the 1990's [39], uses the principle of low-coherence interferometry to generate 3-D reconstructions of the retina and is rapidly becoming a standard. Even though we do not consider OCT images in this paper, most methods of image analysis discussed in this paper apply to OCT data with minor changes.

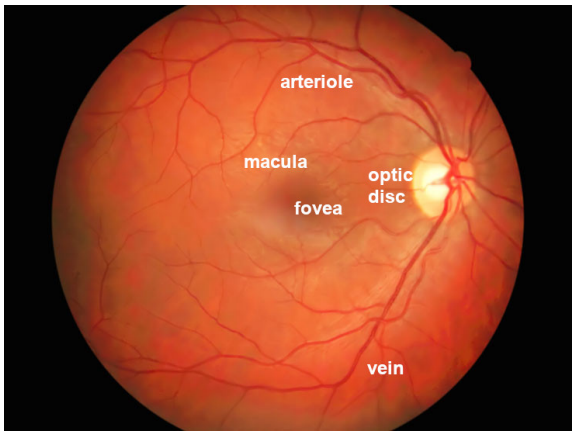

Fig. 2 Retinal circulation visualized through fluorescein angiography. Fluorescein angiography is a medical procedure in which a fluorescent contrast dye is injected into the bloodstream. The dye highlights the blood vessels located in the back of the eye (the ocular fundus) so that they can be visualized and photographed.

2.4 Image Dataset

To facilitate the development fundus image analysis methods and provide benchmark against which to compare the performance of different algorithms, a number of research groups have created publicly available, annotated fundus image databases. The most notable are the following.

- MESSIDOR database [71]. It includes 1200 color fundus images taken with resolutions ranging from 1440×960 pixels to 2304×1536 pixels [51]. Each image is categorized in one of four groups, corresponding to a diabetic patients without diabetic retinopathy and three increasing stages of diabetic retinopathy.
- DRIVE database [33]. It was established to enable comparative studies on segmentation of retinal blood vessels in fundus images. It contains 40 fundus images

of size 768×584 pixels from subjects with diabetes, of which 7 show signs of diabetic retinopathy and the rest appear healthy. The set is divided into a training and a test set, both containing 20 images. For the training images, a manual segmentation of the vasculature is available (see Figure 3). For the test cases, two manual segmentations are available; one given as gold standard, the other one given to compare computer generated segmentations with those of an independent human observer.

- STARE database [93]. This database contains 402 retinal fundus images annotated by domain experts for 44 possible manifestations (features) visible in each image. Manual segmentation of the vasculature is also included for a subset of 40 images of size 605×700.
- HRF database [50]. It contains 45 color fundus images divided into 15 images of healthy patients, 15 images of patients with diabetic retinopathy and 15 images of patients with glaucoma. These images were acquired using a Canon CR-1 fundus camera with a field of view of 60 degrees and have a size of 3504×2336 pixels. The database also includes a manual segmentation of the vessel network performed by human experts.

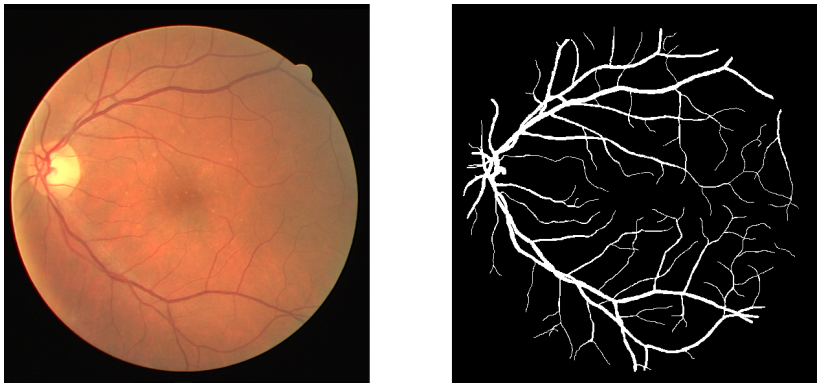

Fig. 3 Representative fundus image (right) from the DRIVE image database and corresponding manual segmentation (right) also available in the database.

3 Automated image analysis of retinal vascularization

Characteristics of the retinal vascular structure are potential indicators of various diseases and the first attempts to automatically extract quantitative information that could be relevant for clinical diagnostics can be traced back to the pioneering work of Matsui et al. [69]. Spurred by the emergence of digital retinal photography and digital filter-based image analysis techniques, retinal image processing developed

dramatically in the 1990s. These developments resulted in a large number of publications focusing on the digital reconstruction of retinal vessel and quantification of local vessel characteristics such as vessel width and branching angles or global ones such as the fractal dimension of the whole vessel network. Many such studies, though, especially before the year 2000, were mostly descriptive; while they did establish an association between local or global changes of retinal vascularization and a disease, they could not predict the presence of a disease based on observed vascular changes. Only during the last 10-15 years, with the emergence of methods from machine learning, an increasing number of publications did focus on applying measures of retinal vascularization to disease prediction and biomarkers discovery.

Together with such advances, studies during the last decade have established that alterations in retinal vascularization are not only associated with eye diseases, but also with cardiovascular and brain diseases since changes in retinal microvasculature may reflect similar changes occurring in blood flow dynamics and cerebral microvasculature. Since retinal vessels are the only segment of the human microcirculation that can be observed directly, these discoveries have further motivated the effort in developing computerized methods of retinal image analysis capable of predicting the insurgence of cardiovascular diseases such as hypertension [27, 101] or cerebral disease such as AD [16, 29, 48].

Below, we survey classical and state-of-the-art results in this active area of investigation.

3.1 Local measures of retinal vascularization

Several classical studies have focused on extracting local measurements from retinal fundus images. To generate objective measures so that images from different patients can be compared, the effect of image magnification due to the photographic acquisition has to be removed either by taking the magnification into account or by defining dimensionless measurements. We list below local measurements most commonly found in the literature.

Retinal vessel width or caliber. Several algorithms have proposed methods to extract retinal vessel width automatically or semi-automatically [20, 40]. A number of papers have investigated the relevance of retinal vascular caliber and its variability in connection with diabetic retinopathy and hypertension [21, 56, 74, 85, 96]. However fundus images are subject to magnification and affected by potential refractive error so that measurements recorded from any particular individual cannot be directly compared with another individual. Hence, alternative dimensionless measurements have been proposed, most notably the arteriolar–venular ratio (AVR) and the length-diameter ratio.

Arteriolar-venular ratio. It is defined as the ratio between the average diameters of the arterioles with respect to the venules and was first proposed by Stokoe and Turner [94] in connection with the study of vascular changes in patients

undergoing treatment for hypertension. This quantity has been further investigated for its potential association with cardiovascular disease [58, 103].

Length-diameter ratio. It is calculated as the length from the midpoint of a particular vascular bifurcation to the midpoint of the preceding bifurcation, expressed as a ratio to the diameter of the parent vessel at the bifurcation. This is another dimensionless measure that is affected by changes in vascular calibre and has been found to be increased in hypertension [55].

Angles at vessel bifurcations. Another measurable parameter of blood vessel topography is the angle subtended between two branching offspring blood vessels at a bifurcation junction. Studies have shown that this angle is reduced in hypertension [92].

Junctional exponents. It is defined as the X exponent in the mathematical relationship $D_0^X = D_1^X + D_2^X$, where D_0 is the diameter of the parent vessel, D_1 and D_2 are the diameters of the offspring vessels. This expression is based on the physical observation that arterial diameters at any bifurcation should conform to a relationship that minimizes shear stress in a vascular network [105]. The junctional exponent has been calculated to be approximately equal to $X = 3$ when vascular network costs are minimized and this value has been confirmed experimentally [106]. Studies have shown that retinal junctional exponents deviate from optimal values with advancing age and hypertension [92], and in association with vascular disease [19].

Vessel tortuosity. This parameter is the subject of multiple studies and several definitions are proposed in the literature [1, 83]. Even though there is no unique definition, it is often defined as the ratio between the length of a vessel from A to B and the shortest distance between points A and B drawn by a straight line. The degree of vascular tortuosity has been associated with a number of vascular and nonvascular diseases such as diabetic retinopathy, cerebrovascular disease, stroke, and ischemic heart disease [25, 26, 88] and has been used as a measure of disease severity in retinopathy of prematurity. [25, 100].

Neovascolarization. It describes the sprouting of new vessels from pre-existent ones and has been associated with aging and eye disease as age-related macular degeneration [18].

3.2 Global measures of retinal vascularization

Since individual local measures of retinal vascularization do not convey sufficient information to capture the complexity of the retinal vascular branching pattern and since many diseases have been observed to be associated with a general microvascular remodeling of the retina, several studies have proposed methods to quantify the overall geometric complexity of retinal vasculature.

Fractal analysis. A large number of papers have proposed the use of fractal geometry to measure the pattern characteristics of the retinal vascular branches; in a Google Scholar search, we found 174 publications whose titles contain the

Subgroup	Mean ± STD		
	Tortuosity Measure [13]	Orientation Score [90]	Fractal Dimension [53]
R0	1.624 ± 0.120	0.0866 ± 0.0166	1.3864 ± 0.0324
R1	1.657 ± 0.124	0.0885 ± 0.0156	1.3852 ± 0.0345
R2	1.698 ± 0.122	0.0894 ± 0.0160	1.3781 ± 0.0364
R3	1.795 ± 0.160	0.0930 ± 0.0163	1.3869 ± 0.0384

Table 1 Average value of Tortuosity Measure [13], Orientation Score [90] Fractal Dimension [53] on the MESSIDOR dataset. Data consists of 4 subgroups, R0-R3, where R0 are the healthy cases and R1-R3 are diabetic retinopathy cases in increasing degree of severity. Representative images from the MESSIDIOR dataset for the 4 subgroups are shown in Fig. 4.

words 'retinal' and 'fractal'. Central to such methods is the concept of fractal dimension D that provides a quantitative measure of the degree of complexity of a geometric set as a ratio of the change in detail to the change in scale [66]. For a classical rectifiable curve f, we have that $D(f) = 1$ (matching its topological dimension) while, for more irregular curves, $D(f) > 1$ and $D(f) = 2$ if a curve is plane-filling curve. Family, Masters and Platt [35, 67] were the first to introduce fractal analysis to quantify retinal vascular branching patterns and found that, in normal retina, $D(f) \simeq 1.7$ in accord with the theoretical diffusion limited aggregation model by Witten and Sander [102]. Following this work, other studies observed that larger fractal dimension of the retinal vasculature, reflecting higher geometric complexity of the retinal vascular branching pattern, is associated with early signs of retinopathy [22] and that lower fractal dimension, reflecting reduction in the retinal vasculature complexity, is observed with aging [9, 10]. Without attempting to list all contributions to this topic, we recall that changes in retinal vascular fractal dimension have been shown also to be related to hypertension [24, 28, 109], stroke [9, 23, 31, 57] and mortality from coronary heart disease [61].

However, the measurement of the fractal dimension of retinal vessels is very sensitive to image quality and the method used for its computation [53]. In addition, studies have shown that the fractal dimension alone is unable to differentiate vasculatures with very similar fractal dimension but different structures in their fluid dynamic design and function [53, 107] and that additional information is needed to assess the pathological vascular states [68]. To overcome this limitation, researchers in the field have proposed more sophisticated tools from fractal geometry including the notion of Fourier Fractal dimension [9] and the application multifractal analysis where the fractal dimension D is replaced by a measure consisting of a vector providing a more accurate description of the underlying geometry [95, 97, 98]. Yet another recent approach combines fractal analysis with graph-based method [6] where first a graph is extracted from the retina blood vessel structure with the nodes representing branching or end points and the edges representing vessel segments; fractal analysis is then used to characterize the extracted graphs.

Orientation measures. With the emergence of advanced multiscale methods about 2005, a number of researchers proposed methods to analyze and quantify retinal

vessel networks based on multiscale directional representations. Among such contributions, we recall in particular the work by Bekkers et al. [13, 49] that applies a sophisticated geometric approach based on theory of best exponential curve fits in the roto-translation group to define a new tortuosity measure. We also recall the work by Sing et al. [90] that applies a system of multiscale directional filters inspired by the theory of shearlets to generate a measure of vessel organization called *orientation score*. Even though the orientation score was originally applied for the analysis of neuronal images, the same method can be applied directly on retinal images [51]. We report in Table 1 the application of these measures to the analysis of fundus images on the MESSIDOR dataset. The table shows that, as compared with the fractal dimension, these alternative geometric measures provide a more insightful description of the changes in retinal vasculature associated with diabetic retinopathy.

Machine learning methods. During the last decade, several research teams have applied methods from machine learning for the automated detection of retinal diseases on fundus images taken from databases or retinal screening programs [8, 17]. The basic idea in such studies consists in extracting features from retinal images and then apply supervised classifiers such as support vector machines (SVM), random forests or naive Bayes classifiers to separate images into distinct pathological classes, such as healthy and diabetic retinopathy cases. Typically these studies extract a multiplicity of retinal image features that include both vasculare features, such as vessel width and fractal dimension, and non-vascular ones, such as lesions, exudates and hemorrhages (cf. [4, 7, 82, 86]).

More recently, following the spectacular success of deep learning algorithms in many classification tasks, an increasing number of studies is applying deep learning algorithms, especially Convolutional Neural Networks (CNN), to predict the presence of a disease in fundus images. One major difference with respect to more traditional machine learning methods is that deep learning algorithms learn features directly from the raw images avoiding the use of hand-designed or model-based features [89]. While these algorithms typically require a relatively large number of training (labeled) samples to learn a satisfactory model of the disease class, they are more flexible than conventional machine learning methods and – when properly trained – can perform very competitively. However, the need of many training samples can be a serious limitation in the clinical application of this approach [30].

Similar to classification using traditional machine learning, also the features learned by the deep learning algorithms are usually not limited to vascular features. In most cases, even though the algorithm is not designed to explicitly detect lesions (e.g., hemorrhages, microaneurysms), it implicitly learns to recognize them when it extracts local features [41, 46]. In some applications, the deep learning approach is explicitly designed to detect lesions [3]. However, one can apply a deep learning framework to efficiently learn features of retinal vascularization by using a representation learning approach, as recently proposed by Giancardo et al. [44]. Their approach generates a vasculature embedding by lever-

Publication	Features	Classifier	AUC
Antal et al. (2014) [7]	Lesions + anatomy	Ensemble	0.989
Gargeya et al. [41] (2017)	Deep features	CNN	0.940
Giancardo et al. (2017) [44]	Vasculature embedding	SVM	0.678
Giancardo et al. (2017) [44]	Vasculature embedding + microaneurysms	SVM	0.865
Roychowdhury et al. (2014) [86]	Lesions + anatomy	Hierarchical	0.904

Table 2 Diabetic retinopathy classification performance – measured in AUC – on the MESSIDOR dataset using different classification methods. Images are classified into 2 classes as healthy vs diabetic retinopathy.

aging the internal representation of a specially designed CNN trained end-to-end with the raw pixels and manually segmented vessels.
Table 2 compares the classification performance of multiple machine learning and deep learning algorithm on the MESSIDOR dataset where images are assigned either to the healthy or to the diabetic retinopathy class. Performance metric is the area under the curve (AUC) obtained by measuring the area under the receiver operating characteristic (ROC) curves that is created by plotting the true positive rate against the false positive rate at various threshold settings.

3.3 Segmentation of retinal vessels

Automated segmentation of the vascular network in fundus images is a nontrivial task due to the variable size of the vessels, the relative low intensity contrast and the possible occurrence of abnormalities such as haemorrhages and microaneurysms [15]. Over the last approximately 20 years, this topic has been the subject of a large number of studies with over a hundred publications including several excellent reviews [5, 38, 75]. In general, existing algorithms for the segmentation of the vascular network in fundus images can be divided into two groups. The first one consists of unsupervised or rule-based methods that include morphological operators [36, 70], adaptive thresholding [54], variational methods [87, 108], vessel-tracking [12, 104], multiscale and/or orientable filters [11, 34, 47, 60, 72]. The second group consists of supervised methods (which require manually labelled images for training) and includes classical methods of machine learning and pattern recognition [37, 64, 84, 91] as well as several methods appeared during the last few years based on convolutional neural networks [52, 62, 76, 77, 99].

To date retinal vessel segmentation in fundus images is a generally well understood problem [73]. The field did benefit enormously from the availability of annotated images in several publicly available databases that made it possible to develop and compare the performance of various algorithms.

Table 3 compares the segmentation performance of multiple traditional and state of the art strategies evaluated on DRIVE. Performance is assessed using the standard metrics of Sensitivity (Se) or Recall, Specificity (Sp) and Dice similarity coefficient (DSC) or F1 score defined below. By comparing the algorithm pixel classification

Publication	Se	Sp	AUC	DSC
Unsupervised				
Azzopardi et al. (2015) [11]	0.7655	0.9704	0.9614	-
Fraz et al. (2011) [36]	0.7152	0.9768	-	0.7642
Miri et al. (2010) [72]	0.7352	0.9795	0.9458	-
Roychowdhury et al. [87]	0.7249	0.9830	0.9620	-
Zhao et al. (2015) [108]	0.7420	0.9820	-	-
Supervised				
Liskowski et al. (2016) [62]	0.7520	0.9806	0.9710	-
Lupascu et al. (2010) [64]	0.6728	0.9874	0.9561	-
Oliveira et al. (2018) [76]	0.8039	0.9804	0.9821	-
Orlando et al. (2017) [77]	0.7897	0.9684	0.9506	0.7857
Soares et al. (2010) [91]	0.7283	0.9788	0.9614	-
Vega et al. (2015) [99]	0.7444	0.9600	-	0.6884

Table 3 Retinal blood vessels segmentation performance – measured in Sensitivity (Se) , Specificity (Sp), AUC and Dice similarity coefficient (DSC) – on the DRIVE dataset using different supervised and unsupervised algorithms.

with respect to the gold standard labeling (manual segmentation), we determine the number of true positives (TP), true negatives (TN), false positives (FP) and false negatives(FN). Then we obtain

$$Se = \frac{TP}{TP + FN}, \quad Sp = \frac{TN}{TN + FP},, \quad DSC = \frac{2TP}{2TP + FP + FN}.$$

Sensitivity measures the ability of the method to properly detect blood vessels, while specificity measures its capability of distinguishing the other non-vessel structures. DSC is a measure of the overall performance of the algorithm. It achieves its maximum value of 1 when the segmentation o is perfect and its lowest value of 0 when the segmentation is completely wrong.

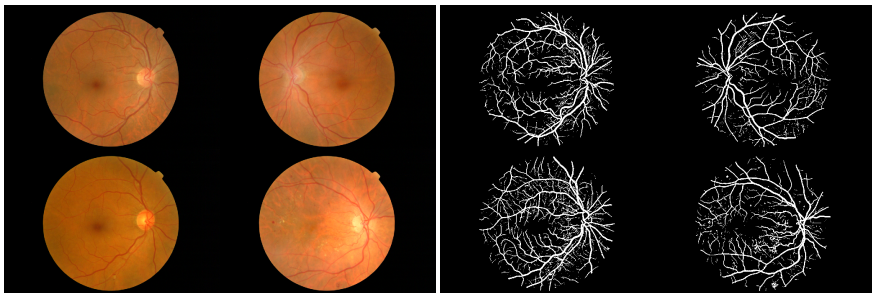

Fig. 4 Left panel: Representative images from MESSIDOR dataset. Starting from top left, clockwise: healthy retina, low-degree retinopathy, medium-degree retinopathy, high-degree retinopathy. Right panel: corresponding segmented images obtained from the B-Cosfire algorithm [11].

Acknowledgements M.C. acknowledges the hospitality of the Department of Mathematics at the University of Houston where this work was initiated. D.L. acknowledges partial support of NSF DMS 1720487 and 1720452.

References

1. M. Abdalla, A. Hunter, B. Al-Diri. Quantifying retinal blood vessels' tortuosity. *2015 Science and Information Conference (SAI)* (2015), 687-693.
2. M.D. Abramoff, M.K. Garvin, M. Sonka. Retinal imaging and image analysis. *IEEE reviews in biomedical engineering* **3** (2010), 169-208.
3. M.D. Abramoff, Y. Lou, A. Erginay, W. Clarida, R. Amelon, J.C. Folk, M. Niemeijer. Improved automated detection of diabetic retinopathy on a publicly available dataset through integration of deep learning. *Investigative ophthalmology & visual science* **57**(13) (2016), 5200-5206.
4. R. Acharya, C.K. Chua, E.Y.K. Ng, W. Yu, C. Chee. Application of higher order spectra for the identification of diabetes retinopathy stages. *Journal of Medical Systems* **32** (6) (2008), 481-488.
5. J. Almotiri, K. Elleithy, A. Elleithy. Retinal Vessels Segmentation Techniques and Algorithms: A Survey. *Applied Sciences* **8**(2) (2018), 155.
6. P. Amil, C.F. Reyes-Manzano, L. Guzman-Vargas, I. Sendina-Nadal, C. Masoller. Network-based features for retinal fundus vessel structure analysis. *PloS one* **14**(7) (2019).
7. B. Antal, A. Hajdu. An ensemble-based system for automatic screening of diabetic retinopathy. *Knowledge-based systems* **60** (2014), 20-27.
8. N. Asiri, M. Hussain, F. Al Adel, N. Alzaidi. Deep Learning based Computer-Aided Diagnosis Systems for Diabetic Retinopathy: A Survey. *Artificial intelligence in medicine* (2019).
9. M.C. Azemin, D.K. Kumar, T.Y. Wong, R. Kawasaki, P. Mitchell, J.J. Wang. Robust methodology for fractal analysis of the retinal vasculature. *IEEE transactions on medical imaging* **30**(2) (2011), 243-250.
10. M.C. Azemin, D.K. Kumar, T.Y. Wong, R. Kawasaki, P. Mitchell, J.J. Wang. Age-related rarefaction in the fractal dimension of retinal vessel. *Neurobiol Aging* **33** (2012), 194.e1–194.e4.
11. G. Azzopardi, N. Strisciuglio, M. Vento, and N. Petkov. Trainable cos-fire filters for vessel delineation with application to retinal images. *Medical image analysis* **19** (2015), 46–57.
12. E. Bekkers, R. Duits, T. Berendschot, B. ter Haar Romeny. A multi-orientation analysis approach to retinal vessel tracking. *Journal of Mathematical Imaging and Vision* **49**(3) (2014), 583-610.
13. E. Bekkers, J. Zhang, R. Duits, B. ter Haar Romeny. Curvature based biomarkers for diabetic retinopathy via exponential curve fits in SE(2). *Proceedings of the Ophthalmic Medical Image Analysis Second International Workshop*, OMIA 2015, Held in Conjunction with MICCAI 2015, 113–120.
14. R. Bernardes, P. Serranho, C. Lobo. Digital ocular fundus imaging: a review. *Ophthalmologica* **226**(4) (2011), 161-181.
15. P.F.C. Breda. Deep Learning for the Segmentation of Vessels in Retinal Fundus images and its Interpretation. *Ph.D. Thesis, Faculdade de Engenharia da Universidade do Porto*, October 2018.
16. D. Cabrera DeBuc, G.M. Somfai, A. Koller. Retinal microvascular network alterations: potential biomarkers of cerebrovascular and neural diseases. *American Journal of Physiology-Heart and Circulatory Physiology* **312**(2) (2016), H201-H212.
17. M. Caixinha, S. Nunes. Machine learning techniques in clinical vision sciences. *Current eye research* **42**(1) (2017), 1-15.
18. P.A. Campochiaro. Ocular neovascularization. *Journal of molecular medicine* **91**(3) (2013), 311-321.

19. N. Chapman, G. Dell'omo, M.S. Sartini, N. Witt, A. Hughes, S. Thom, R. Pedrinelli. Peripheral vascular disease is associated with abnormal arteriolar diameter relationships at bifurcations in the human retina. Clinical Science **103** (2002), 111–116.
20. N. Chapman, N. Witt, X. Gao, A.A. Bharath, A.V. Stanton, S. Thom, A.Hughes. Computer algorithms for the automated measurement of retinal arteriolar diameters. *Br. J. Ophthalmol.* **85** (2001), 74–79.
21. N. Cheung, S.L. Rogers , K.C. Donaghue, A.J. Jen-kins, G. Tikellis, T.Y. Wong. Retinal arteriolar dilation predicts retinopathy in adolescents with type 1 diabetes. *Diabetes Care* **31** (2008), 1842–1846.
22. N. Cheung, K.C.Donaghue, G. Liew, S.L. Rogers, J.J. Wang, S.W. Lim, A.J.Jenkins, W. Hsu, M.L. Lee and T.Y. Wong. Quantitative assessment of early diabetic retinopathy using fractal analysis. *Diabetes care* **32**(1) (2009), 106-110.
23. N. Cheung, G. Liew, R.I Lindley, E.Y. Liu, J.J. Wang, P. Hand, M. Baker, P. Mitchell and T.Y. Wong. Retinal fractals and acute lacunar stroke. *Annals of neurology* **68**(1) (2010), 107-111.
24. C.Y. Cheung, W.T. Tay, P. Mitchell, J.J. Wang, W. Hsu, M.L. Lee, Q.P. Lau, A.L. Zhu, R. Klein, S.M. Saw and T.Y. Wong. Quantitative and qualitative retinal microvascular characteristics and blood pressure. *Journal of hypertension* **29**(7) (2001), 1380-1391.
25. C.S. Cheung, Z. Butty, N.N. Tehrani and W.C. Lam. Computer-assisted image analysis of temporal retinal vessel width and tortuosity in retinopathy of prematurity for the assessment of disease severity and treatment outcome. *Journal of American Association for Pediatric Ophthalmology and Strabismus* **15**(4) (2011), 374-380
26. C.Y.L. Cheung, Y. Zheng, W. Hsu, M.L. Lee, Q.P. Lau, P. Mitchell, J.J. Wang, R. Klein and T.Y. Wong. Retinal vascular tortuosity, blood pressure, and cardiovascular risk factors. *Ophthalmology* **118** (5) (2011), 812-818
27. C.Y. Cheung, M.K. Ikram,C. Sabanayagam, T.Y. Wong. Retinal microvasculature as a model to study the manifestations of hypertension. *Hypertension* **60** (5) (2012), 1094–1103.
28. C.Y. Cheung, G.N. Thomas, W. Tay, M.K. Ikram, W. Hsu, M.L. Lee, Q.P. Lau and T.Y. Wong. Retinal vascular fractal dimension and its relationship with cardiovascular and ocular risk factors. *American journal of ophthalmology* **154** (4) (2012), 663-674.
29. C.Y.L. Cheung, Y.T. Ong, M.K. Ikram, S.Y. Ong, X. Li, S. Hilal, J.A.S. Catindig, N. Venketasubramanian, P. Yap, D. Seow and C.P. Chen. Microvascular network alterations in the retina of patients with Alzheimer's disease. *Alzheimer's & Dementia* **10** (2) (2014), 135-142.
30. J.Y. Choi, T.K. Yoo, J.G. Seo, J. Kwak, T.T. Um and T.H. Rim. Multi-categorical deep learning neural network to classify retinal images: A pilot study employing small database. *PloS one* **12**(11) (2017), p.e0187336.
31. F.N. Doubal, T.J. MacGillivray, N. Patton, B. Dhillon, M.S. Dennis, J.M. and Wardlaw. Fractal analysis of retinal vessels suggests that a distinct vasculopathy causes lacunar stroke. *Neurology* **74** (14) (2010), 1102-1107.
32. J. E. Dowling. The retina: an approachable part of the brain. *Harvard University Press* (1987).
33. DRIVE database. https://computervisiononline.com/dataset/1105138662
34. M. Esmaeili, H. Rabbani, A. Mehri and A. Dehghani. Extraction of retinal blood vessels by curvelet transform. *In 2009 16th IEEE International Conference on Image Processing (ICIP)* (2009), 3353-3356.
35. F. Family, B. Masters, D. Platt. Fractal pattern formation in human retinal vessels. *Physica D: Nonlinear Phenomena* **38** (1989), 98–103.
36. M.M.Fraz, P. Remagnino, A. Hoppe, B. Uyyanonvara, C.G. Owen, A.R. Rudnicka and S.A Barman. Retinal vessel extraction using first-order derivative of Gaussian and morphological processing. *In International Symposium on Visual Computing* (2011), 410-420. Springer, Berlin, Heidelberg.
37. M. M. Fraz, P. Remagnino, A. Hoppe, B. Uyyanonvara, A. R. Rudnicka,C. G. Owen, and S. A. Barman, An ensemble classification-based approach applied to retinal blood vessel segmentation, *IEEE Transactionson Biomedical Engineering* **59** (2012), 2538–2548.
38. M.M. Fraz, P. Remagnino, A. Hoppe, B. Uyyanonvara, A.R. Rudnicka, C.G. Owen and S.A. Barman. Blood vessel segmentation methodologies in retinal images – a survey. *Computer methods and programs in biomedicine* **108**(1) (2012), 407-433.

39. J. G. Fujimoto, C. Pitris, S.A. Boppart, M.E. Brezinski. Optical coherence tomography: an emerging technology for biomedical imaging and optical biopsy. *Neoplasia* **2** (1-2)(2000), 9–25.
40. L. Gang, O. Chutatap and S.M.Krishnan. Detection and measurement of retinal vessels in fundus images using amplitude modified second-order Gaussian filter. *IEEE transactions on Biomedical Engineering* **49** (2) (2002), 168-172.
41. R. Gargeya, T. Leng. Automated identification of diabetic retinopathy using deep learning. *Ophthalmology* **124**(7) (2017), 962-969.
42. O. Gerloff. Über die Photographie des Augenhintergrundes. *Klin Monatsblätter Augenheilkunde* **29** (1891), 397–403.
43. L. Giancardo. Automated fundus images analysis techniques to screen retinal diseases in diabetic patients. *Ph.D. Thesis, Universit e de Bourgogne* (2011).
44. L. Giancardo, K. Roberts, Z. Zhao. Representation learning for retinal vasculature embeddings.*Fetal, Infant and Ophthalmic Medical Image Analysis* (2017), 243-250.
45. A. Gullstrand. Neue methoden der reflexlosen ophthalmoskopie. *Berichte Deutsche Ophthalmologische Gesellschaft* **36** (1910).
46. V. Gulshan, L. Peng, M. Coram, M.C. Stumpe, D. Wu, A. Narayanaswamy, S. Venugopalan, K. Widner, T. Madams, J. Cuadros and R. Kim. Development and validation of a deep learning algorithm for detection of diabetic retinopathy in retinal fundus photographs. *Jama* **316**(22) (2016), 2402-2410.
47. Y. Guo, U. Budak, A. Şengür, F. Smarandache. A retinal vessel detection approach based on shearlet transform and indeterminacy filtering on fundus images. *Symmetry* **9**(10) (2017), 235.
48. J. den Haan, J.A. van de Kreeke, B.N. van Berckel, F. Barkhof, C.E. Teunissen, P. Scheltens, F.D. Verbraak, F.H. Bouwman. Is retinal vasculature a biomarker in amyloid proven Alzheimer's disease?. *Alzheimer's & Dementia: Diagnosis, Assessment & Disease Monitoring* **11** (2019), 383-391.
49. B.M. ter Haar Romeny, E.J. Bekkers, J. Zhang, S. Abbasi-Sureshjani, F. Huang, R. Duits, B. Dashtbozorg, T.T. Berendschot, I. Smit-Ockeloen, K.A. Eppenhof and J. Feng. Brain-inspired algorithms for retinal image analysis. *Machine Vision and Applications* **27**(8) (2016), 1117-1135.
50. HREF database. https://www5.cs.fau.de/research/data/fundus-images/
51. S. Hoteit, Quantitative methods in retinal fundus imaging. *Doctoral dissertation. Department of Mathematics of the University of Houston*. May 2020.
52. K. Hu, Z. Zhang, X. Niu, Y. Zhang, C. Cao, F. Xiao and X. Gao. Retinal vessel segmentation of color fundus images using multiscale convolutional neural network with an improved cross-entropy loss function. *Neurocomputing* **309** (2018), 179-191.
53. F. Huang, B.Dashtbozorg, J. Zhang, E. Bekkers, S. Abbasi-Sureshjani, T.T. Berendschot and B.M. ter Haar Romeny. Reliability of using retinal vascular fractal dimension as a biomarker in the diabetic retinopathy detection. *Journal of ophthalmology* (2016).
54. X. Jiang, D. Mojon. Adaptive local thresholding by verification-based multithreshold probing with application to vessel detection in retinal images. *IEEE Trans. Pattern Anal. Mach. Intell* **25** (2003), 131–137.
55. L.A. King, A.V. Stanton, P.S. Sever, S.A. Thom and A.D. Hughes. Arteriolar length-diameter (L: D) ratio: a geometric parameter of the retinal vasculature diagnostic of hypertension. *Journal of human hypertension* **10**(6) (1996), 417-418.
56. M.K. Ikram, J.C. Witteman, J.R. Vingerling, M.M. Breteler, A. Hofman and P.T. de Jong. Retinal vessel diameters and risk of hypertension: the Rotterdam Study. *Hypertension* **47**(2) (2006), 189-194.
57. R. Kawasaki, M.Z. Che Azemin, D.K. Kumar, A.G. Tan, G. Liew, T.Y. Wong, P. Mitchell, J.J. Wang. Fractal dimension of the retinal vasculature and risk of stroke: a nested case-control study. *Neurology* **76** (2011), 1766–1767.
58. R. Klein, A.R. Sharrett, B.E. Klein, L.E. Chambless, L.S. Cooper, L.D. Hubbard and G. Evans. Are retinal arteriolar abnormalities related to atherosclerosis? The Atherosclerosis Risk in Communities Study. *Arteriosclerosis, thrombosis, and vascular biology* **20**(6) (2000), 1644-1650.

59. H. Kolb. How the retina works. *American scientist* **91**(1) (2003), 28-35.
60. F. Levet, M.A. Duval-Poo, E. De Vito and F. Odone. Retinal Image Analysis with Shearlets. *In Eurographics Italian Chapter Conference* (2016), 151-156).
61. G. Liew, P. Mitchell, E. Rochtchina, T.Y. Wong, W. Hsu, M.L. Lee, A. Wainwright and J.J. Wang. Fractal analysis of retinal microvasculature and coronary heart disease mortality. *European heart journal* **32)**(4) (2010), 422-429.
62. P. Liskowski, K. Krawiec. Segmenting retinal blood vessels with deep neural networks, *IEEE Transactions on Medical Imaging* **35**(11) (2016), 2369–2380.
63. A. London, I. Benhar and M. Schwartz. The retina as a window to the brain—from eye research to CNS disorders. *Nature Reviews Neurology* **9**(1) (2013), 44.
64. C.A. Lupascu, D. Tegolo and E. Trucco. FABC: retinal vessel segmentation using AdaBoost. *IEEE Transactions on Information Technology in Biomedicine* **14**(5) (2010), 1267-1274.
65. T.J. MacGillivray, E. Trucco, J.R. Cameron, B. Dhillon, J.G. Houston, and E.J.R. Van Beek. Retinal imaging as a source of biomarkers for diagnosis, characterization and prognosis of chronic illness or long-term conditions. *The British journal of radiology* **87**(1040) (2014), p.20130832.
66. B. Mandelbrot. How Long is the Coast of Britain? Statistical Self-Similarity and Fractional Dimension. *Science* **156**(3775) (1967), 636–638.
67. B. Masters, D. Platt. Development of human retinal vessels: a fractal analysis. Invest. *Ophthalmol. Vis. Sci.* 30 (Suppl.)(1989), 391.
68. B.R. Masters. Fractal analysis of the vascular tree in the human retina. *Annu Rev Biomed Eng.* **6** (2004), 427–452.
69. M. Matsui, T. Tashiro, K. Matsumoto and S. Yamamoto. A study on automatic and quantitative diagnosis of fundus photographs. i. detection of contour line of retinal blood vessel images on color fundus photographs (author's transl). *Nippon Ganka Gakkai Zasshi* **77**(8) (1973), 907.
70. M. Mendonca and A. Campilho, "Segmentation of retinal blood ves-sels by combining the detection of centerlines and morphological recon-struction. *IEEE Transactions on Medical Imaging* **25** (2006), 1200–1213.
71. MESSIDOR database. http://www.adcis.net/en/third-party/messidor/
72. M.S. Miri and A. Mahloojifar. Retinal image analysis using curvelet transform and multistructure elements morphology by reconstruction. *IEEE Transactions on Biomedical Engineering* **58**(5) (2010), 1183-1192.
73. S. Moccia, E.D. Momi, S.E. Hadji and L.S. Mattos. Blood vessel segmentation algorithms—review of methods, datasets and evaluation metrics. *Computer methods and programs in biomedicine* **158** (2018), 71-91.
74. T.T. Nguyen, J.J. Wang, A.R. Sharrett, F.M. Islam, R. Klein, B. E. Klein, M.F. Cotch, T.Y. Wong. The relationship of retinal vascular caliber with diabetes and retinopathy: the Multi-Ethnic Study of Atherosclerosis (MESA). *Diabetes Care***31**(3) (2008), 544 –549.
75. J. Niemeijer, J. Staal, B. van Ginneken, M. Loog and M. Abramoff. Comparative study of retinal vessel segmentation methods on a new publicly available database. *SPIE Medical Imaging* (J. M. Fitzpatrick and M. Sonka, eds.)**5370** (2004), 648–656.
76. A. Oliveira, S. Pereira and C.A. Silva. Retinal vessel segmentation based on fully convolutional neural networks. *Expert Systems with Applications***112** (2018), 229-242.
77. J. I. Orlando, E. Prokofyeva, M. B. Blaschko. A discriminativelytrained fully connected conditional random field model for bloodvessel segmentation in fundus images. *Transactions on Biomedical Engineering* **64**(1) (2017), 16–27.
78. C.W. Oyster. The human eye. Sunderland, MA, Sinauer (1999).
79. N. Patton, T. Aslam, T. MacGillivray, A. Pattie, I.J. Deary and B. Dhillon. Retinal vascular image analysis as a potential screening tool for cerebrovascular disease: a rationale based on homology between cerebral and retinal microvasculatures. *Journal of anatomy* **206**(4) (2005), 319-348.
80. N. Panwar, P. Huang, J. Lee, P. A. Keane, T. S. Chuan, A. Richhariya and R. Agrawal. Fundus Photography in the 21st Century–A Review of Recent Technological Advances and Their Implications for Worldwide Healthcare. Telemedicine journal and e-health : *the official journal of the American Telemedicine Association* **22**(3) (2016), 198–208. doi:10.1089/tmj.2015.0068

81. N. Patton, T.M. Aslam, T. MacGillivray, I.J. Deary, B. Dhillon, R.H. Eikelboom, K. Yogesan and I.J Constable. Retinal image analysis: concepts, applications and potential. *Progress in retinal and eye research* **25**(1) (2006), 99-127.
82. R. Priya ,P. Aruna. SVM and neural network based diagnosis of diabetic retinopathy. *Int J Comput Appl.* **41**(1) (2012), 6–12.
83. L. Ramos, J. Novo, J. Rouco, S. Romeo, M.D. Álvarez and M. Ortega. Retinal vascular tortuosity assessment: inter-intra expert analysis and correlation with computational measurements. *BMC medical research methodology* **18**(1) (2018), 144.
84. E. Ricci and R. Perfetti. Retinal blood vessel segmentation using line op-erators and support vector classification. *IEEE Transactions on MedicalImaging* **26**(10) (2007), 1357–136.
85. S. Rogers, G. Tikellis, N. Cheung, R. Tapp, J. Shaw, P.Z. Zimmet, P. Mitchell,J.J. Wang, T.Y. Wong. Retinal arteriolar caliber predicts incident retinopathy: the Australia Diabetes, Obesity and Lifestyle (Aus-Diab) Study. *Diabetes Care* **31**(4) (2008), 761–763.
86. S. Roychowdhury, D.D. Koozekanani, K. K. Parh. DREAM: diabetic retinopathy analysis using machine learning. *IEEE J Biomed Heal Informatics* **18**(5) (2014), 1717-1728.
87. S. Roychowdhury, D. D. Koozekanani, and K. K. Parhi. Iterative vessel segmentation of fundus images. *IEEE Transactions on Biomedical Engineering* **62**(7) (2015), 1738–1749.
88. M.B. Sasongko, T.Y. Wong, K.C. Donaghue, N. Cheung, A.J. Jenkins, P. Benitez-Aguirre and J.J. Wang. Retinal arteriolar tortuosity is associated with retinopathy and early kidney dysfunction in type 1 diabetes. *American journal of ophthalmology***153** (1) (2012), 176-183.
89. U. Schmidt-Erfurth, A. Sadeghipour, B.S. Gerendas, S.M. Waldstein and H. Bogunović. Artificial intelligence in retina. *Progress in retinal and eye research* **67** (2018), 1-19.
90. P. Singh, P. Negi, F. Laezza, M. Papadakis and D. Labate. Multiscale analysis of neurite orientation and spatial organization in neuronal images. *Neuroinformatics* **14**(4) (2016), 465-477.
91. J.V.B. Soares, J.J.G. Le, R.M. Cesar, H.F. Jelinek and M.J. Cree. Retinal vessel segmentation using the 2-D Gabor wavelet and supervised classification. *IEEE Trans Med Imaging* **25** (10) (2006), 1214–1222.
92. AV Stanton, B. Wasan, A. Cerutti , et al. Vascular network changes in the retina with age and hypertension. *J. Hypertens.* **13** (1955), 1724–1728.
93. STARE database. http://cecas.clemson.edu/ãhoover/stare/
94. N.L. Stokoe, and R.W. Turner. Normal retinal vascular pattern. Arteriovenous ratio as a measure of arterial calibre. *The British journal of ophthalmology* **50**(1) (1966), 21.
95. T. Stosic, B. Stosic. Multifractal analysis of human retinal vessels. *IEEE Trans Med Imaging.* **25**(8) (2006), 1101–1107.
96. C. Sun, J.J. Wang, D.A. Mackey, and T.Y. Wong. Retinal vascular caliber: systemic, environmental, and genetic associations. *Survey of ophthalmology* **54** (1) (2009), 74-95.
97. Ş. Ţălu. Multifractal characterisation of human retinal blood vessels. *Oftalmologia.* **56** (2) (2012), 63–71.
98. Ş. Ţălu, S. Stach, ,D.M. Călugăru, C.A. Lupaşcu, and S.D. Nicoară. Analysis of normal human retinal vascular network architecture using multifractal geometry. *International journal of ophthalmology* **10**(3) (2017), 434.
99. R. Vega, G. Sanchez-Ante, L.E. Falcon-Morales, H. Sossa and E. Guevara. Retinal vessel extraction using lattice neural networks with dendritic processing. *Computers in biology and medicine* **58** (2015), 20-30.
100. D.K. Wallace. Computer-assisted quantification of vascular tortuosity in retinopathy of prematurity (an American Ophthalmological Society thesis). *Transactions of the American Ophthalmological Society* **105** (2007, 594.
101. N. Witt,T.Y. Wong, A.D. Hughes, N. Chaturvedi, B.E. Klein, , R. Evans, M. McNamara, S.A.M. Thom and R. Klein. Abnormalities of retinal microvascular structure and risk of mortality from ischemic heart disease and stroke. *Hypertension* **47** (5) (2006), 975-981.
102. T. Witten, L. Sander. Diffusion-limited aggregation, a kinetic phenomena. *Phys. Rev. Lett.* **47**(19) (1981), 1400–1403.

103. T.Y. Wong, R. Klein, B.E. Klein, J.M. Tielsch, L. Hubbard and F.J. Nieto. Retinal microvascular abnormalities and their relationship with hypertension, cardiovascular disease, and mortality. *Survey of ophthalmology* **46**(1) (2001), 59-80.
104. Y. Yin, M. Adel and S. Bourennane. Retinal vessel segmentation using a probabilistic tracking method. *Pattern Recognition* **45** (4) (2012), 1235-1244.
105. M. Zamir. Optimality principles in arterial branching. *J. Theor. Biol.* **62** (1) (1976), 227–251.
106. M. Zamir ,J. Medeiros ,TK Cunningham. Arterial bifurcations in the human retina. *J. Gen. Physiol.* **74** (4) (1979), 537–548.
107. M. Zamir. Arterial branching within the confines of fractal L-system formalism. *J. Gen. Physiol* **118** (3) (2001), 267–275.
108. Y. Zhao, L. Rada, K. Chen,S.P. Harding, Y. Zheng. Automated vessel segmentation using infinite perimeter active contour model with hybrid region information with application to retinal images. *IEEE Trans Med. Imaging* **34** (9) (2015), 1797–1807.
109. P. Zhu, F. Huang, F. Lin, Q. Li, Y. Yuan, Z. Gao and F. Chen. The relationship of retinal vessel diameters and fractal dimensions with blood pressure and cardiovascular risk factors. *PloS one* **9**(9) (2014), p.e106551.